



On the magnitude and uncertainties of global and regional soil organic carbon: A comparative analysis using multiple estimates

Ziqi Lin¹, Yongjiu Dai¹, Umakant Mishra², Guocheng Wang³, Wei Shangguan¹, Wen Zhang³, Zhangcai Qin¹

¹School of Atmospheric Sciences, Guangdong Province Key Laboratory for Climate Change and Natural Disaster Studies, Sun Yat-sen University, and Southern Marine Science and Engineering Guangdong Laboratory (Zhuhai), Zhuhai 519082, China

²Computational Biology & Biophysics, Sandia National Laboratories, Livermore, CA 94550, United States

³LAPC, Institute of Atmospheric Physics, Chinese Academy of Sciences, Beijing 100029, China

Correspondence to: Zhangcai Qin (qinzhangcai@mail.sysu.edu.cn)

Abstract. Globally, soil is one of the largest terrestrial carbon reservoirs, with soil organic carbon (SOC) regulating overall soil carbon dynamics. Robust quantification of SOC stocks in existing global observation-based estimates avails accurate predictions in carbon climate feedbacks and future climate trends. In this study, we investigated global and regional SOC estimates, based on five widely used global gridded SOC datasets (HWSD, WISE30sec, GSDE, SoilGrids250m, and GSOCmap), a regional permafrost dataset from Mishra et al. (UM2021), and a global-scale soil profile database (the World Soil Information Service soil profile database, WoSIS) reporting measurements of a series physical and chemical edaphic attributes. Our comparative analyses show that the magnitude and distribution of SOC varies widely among datasets, with certain datasets showing region-specific robustness. At the global scale, the magnitude of SOC stocks simulated by GSDE, GSOCmap, and WISE30sec are comparable, while estimates of SoilGrids250m and HWSD are at the upper and lower ends, respectively. Global SOC stocks ranged from 577-1171 Pg C and 1086-2678 Pg C at 0-30 cm and 0-100 cm depth. The spatial distribution of SOC stocks varies greatly among datasets, especially in the northern circumpolar and Tibetan Plateau permafrost regions. In general, the UM2021 and WISE30sec perform better in the northern circumpolar permafrost regions, and GSDE performs better in China. SOC stocks estimated by different datasets also show large variabilities across different soil layers and biomes. Overall, GSOCmap performs well at 0-30 cm depth, while SoilGrids250m and GSDE perform better at multiple depths. Among the five gridded global datasets, SoilGrids250m exhibits a more consistent spatial pattern and depth distribution with WoSIS. Large uncertainties in existing global gridded SOC estimates are generally derived from soil sampling density, diverse sources and mapping methods for soil datasets. We call for future efforts for standardizing soil sampling efforts, cross-dataset comparison, proper validation, and overall global collaboration to improve SOC estimates. The data are available at <https://doi.org/10.6084/m9.figshare.20220234> (Lin et al., 2022).



30 1 Introduction

Soil stores twice the amount of carbon in atmosphere and vegetation combined thus plays a fundamental role in the global carbon cycle (Piao et al., 2009; Bastida et al., 2019). Soil carbon consists of inorganic carbon (SIC) and organic carbon (SOC), and the latter accounts for over 60% of total soil carbon pool (Lal, 2004; Batjes, 1996; Houghton, 2007). Carbon enters soil profiles through organic inputs and leaves soil *via* mainly heterotrophic respiration, both processes can be significantly affected
 35 by natural and anthropogenic perturbations (Yang et al., 2020; Lorenz and Lal, 2022). Due to its large size, a minor change in SOC stock can have profound impacts on atmospheric CO₂ concentration and hence climate change (Ciais et al., 2013; Köchy et al., 2015b). Thus, accurate estimation of SOC is essential for carbon climate feedbacks and future climate change projections. In recent decades, there have been many soil data products, at either global or regional scale, constructed to satisfy diversified demands for soil information (Batjes et al., 2017). At regional and national scales, there are many datasets compiled by local
 40 governments and regional organizations based on regional soil surveys, e.g., the Soil and Terrain databases (SOTER) (van Engelen and Dijkshoorn, 2013), the European Soil Database (ESDB) (Panagos et al., 2012), the 1:100 million scale Soil Map of China (Shi et al., 2004), the Australian Soil Resource Information System polygon attributed surface (ASRIS) (McKenzie et al., 2000), and Africa Soil Information Service (AfSIS) (Leenaars et al., 2014). The global soil datasets are primarily generated by international institutions and organizations, like the Food and Agriculture Organization of the United Nations
 45 (FAO). These organizations first collected soil information from the national and/or regional soil databases, then processed and compiled the information to construct a harmonized global soil dataset. For example, FAO integrated nearly 600 soil maps around the world to compile the World Soil Map (SMW) and then digitized it to build the Digital World Soil Map (DSMW) (FAO, 1974, 1988, 1995). The Harmonized World Soil Database (HWSD) was established by using the regional and national soil information assimilated and harmonized by International Institute for Applied Systems Analysis (IIASA) and FAO (FAO
 50 et al., 2012).

So far, a number of global and regional soil datasets have been produced and used, but they often vary largely in terms of data sources, mapping methods, soil properties, and the purposes and scope. For instance, the ISRIC-WISE-derived soil property databases (Batjes, 2005, 2012, 2016) and the SoilGrids system (Hengl et al., 2014, 2017) differ in data sources and mapping approaches, but they have all been widely used for different studies. The Global Soil Dataset for Earth System Models
 55 (GSDE) (Shangguan et al. 2014) was originally developed for Earth System Models (ESM), and the many soil properties included can well serve as model inputs (Shangguan et al. 2014). By contrast, the Global Soil Organic Carbon Map (GSOCmap) was established to simulate the distribution of global soil organic carbon only (FAO and ITPS, 2018). It should also be noted that many soil data products have been updated from previous soil databases, to deal with problems including data outdated, coarse spatial resolution, and differences in process of soil data. For example, HWSD started on the basis of the framework of



60 DSMW (FAO et al., 2012), complemented soil information, and eventually superseded DSMW. ISRIC-World Soil Information further used the soil profiles from Harmonized continental SOTER-derived database (SOTWIS) (van Engelen et al., 2005) and the International Soil Carbon Network (ISCN) (Nave et al., 2015) to supplement the data missing area of HWSD and constructed WISE30sec.

Previous studies have evaluated SOC estimates of various soil data products from different perspectives. Scharlemann et al. (2014) performed a meta-analysis and reported that global 0-1 m SOC stocks ranged from 504 to 3000 Pg C, with a median of 1460.5 Pg C. Dai et al. (2019) evaluated several existing soil datasets in the application of ESMs. To construct or improve a certain soil data product, many inter-comparisons among different SOC estimates have been done as references (Hiederer and Köchy, 2011; Köchy et al., 2015a; FAO and ITPS, 2018). However, few studies have comprehensively compared and assessed SOC estimates across multiple existing products, identifying knowledge gaps in global and regional SOC magnitude and uncertainties that may differ among datasets. It has been recognized that the high variability in SOC estimates among different studies could be from diverse calculation approaches (Köchy et al., 2015a). Moreover, current global soil datasets are updated frequently and there is no unified standard to assess the accuracy of global soil datasets with different formats, content and resolution. If the uncertainty in SOC estimates is to be reduced, the differences among the databases and the impact of these differences on the SOC estimates should be quantified.

75 In this study, we used five global soil datasets (HWSD, WISE30sec, GSDE, SoilGrids250m and GSOCmap) to quantify the magnitude and distribution of global SOC stocks and its uncertainties at depth of 0-30 cm and 0-100 cm, respectively. We used a regional permafrost dataset developed by Mishra et al. (2021) (called UM2021 in this study) to facilitate comparison in the regions with permafrost. We also used the World Soil Information Service soil profile database (WoSIS) as a reference for comparison purpose. Through the robust quantification of uncertainty in existing global SOC observation-based estimates, we can quantify the magnitude and distribution of SOC stocks among current estimates, then identify areas for future improvements, which could reduce the uncertainty in model projected SOC dynamics, carbon climate feedbacks, and future climate trends.

2 Methods and materials

2.1 Soil datasets

85 In this study, we used five widely used and recently updated global soil datasets with estimates of SOC content or density, i.e., HWSDv1.21 (FAO et al., 2012), WISE30sec (Batjes, 2015, 2016), GSDE (Shangguan et al., 2014), SoilGrids250mv1.0 (Hengl et al., 2017) and GSOCmapv1.5 (FAO and ITPS, 2018) (Table 1). Specifically, the HWSD is one of the most coherent and widely used global soil databases, developed by FAO, IIASA, ISRIC-World Soil Information (ISRIC), Institute of Soil Science,



Chinese Academy of Sciences (ISSCAS), and Joint Research Centre of the European Commission (JRC). It was produced by
 90 linking the regional and national soil properties information to the soil map of the world according to taxonomy-based
 pedotransfer functions. The GSDE and WISE30sec are the improvements over the HWSD. They expanded the spatial coverage
 of soil maps and added more soil profiles. Specifically, using a framework of HWSD, the GSDE supplemented soil information
 from the U.S. General Soil Map (GSM) (USDA-NCSS, 2006), the Soil Landscapes of Canada (SLC, version 3.2) (Soil
 Landscapes of Canada Working Group, 2010), ASRIS, the soil database of China for land surface modeling (Shangguan et al.,
 95 2013), and the SOTWIS of the Indo-Gangetic Plains (Batjes et al., 2004), Jordan (Batjes et al., 2003), and Kenya (Batjes and
 Gicheru, 2004). To satisfy the needs for ESMs inputs, the GSDE included 34 soil properties for 8 depth intervals (up to 2.3 m
 depth). WISE30sec corrected the HWSD by using the Köppen-Geiger climate zone map as the categorical covariate and
 complemented with about 8000 soil profiles from some northern high latitude regions, and estimated 20 soil properties of 7
 layers to a depth of 2 m. For SoilGrids250m, the first version (1.0) was still used here for method consistency between 0-30
 100 cm and 0-100 cm. The latest version (SoilGrids 2.0) was recently released (Poggio et al., 2021), but the data for 0-100 cm SOC
 stocks is unavailable at the moment, and re-analysis by users to derive 0-100 cm SOC stocks could potentially result in
 inconsistent results (personal communication). SoilGrids250m (v1.0) was mapped by machine learning methods based on
 about 150000 soil profiles from the WoSIS database and 158 environmental covariates (Hengl et al., 2017). It estimated 11
 soil properties for 6 depth intervals (up to 2 m depth) at 250 m spatial resolution. The GSOCmap is a country-specific grid soil
 105 database for 0-30 cm SOC density, developed by the Global Soil Partnership (GSP). The GSP collected national SOC data
 generated by the member countries according to the harmonized standards and then filled the gaps by using publicly available
 data or simulations.

Moreover, we used a regional permafrost dataset from Mishra et al. (2021) (called UM2021 in this study) for further
 comparison of the SOC stock in the permafrost affected soils, both in northern circumpolar region and the Tibetan Plateau.
 110 The UM2021 was created by combining over 2700 soil profiles with environmental variables in a geospatial framework. It
 provided the most up-to-date SOC density information and associated uncertainty estimates of permafrost affected soils for 4
 depth intervals at a spatial resolution of 250 m.



Table 1 Key features of soil datasets

Name (version)	HWSD (Version 1.21)	GSDE	WISE30sec	SoilGrids250m (Version 1.0)	GSOCmap (Version 1.5)	UM2021
Number of layers	2	8	7	6	1	4
Depth interval (cm)	30, 100	4.5, 9.1, 16.6, 28.9, 49.3, 82.9, 138.3, 229.6	20, 40, 60, 80, 100, 150, 200	5, 15, 30, 60, 100, 200	30	30, 100, 200, 300
Properties	16	34	20	11	1	1
Spatial Resolution	30" (~1km)	30" (~1km)	30" (~1km)	250m	30" (~1km)	250m
Update time	2012	2014	2016	2017	2018	2021
Domain	Global	Global	Global	Global	Global	The northern circumpolar region and the Tibetan Plateau
Data access	http://web.archive.iiasa.ac.at/Research/LUC/External-World-soil-database/HTML/HWSD_Data.html?sb=4 (last access: 5 July 2022)	https://data.isric.org/geonetwork/srv/eng/catalog.search#/metadata/dc7b283a-8f19-45e1-aaed-e9bd515119bc (last access: 5 July 2022)	http://globalchange.bnu.edu.cn/research/soilw (last access: 5 July 2022)	https://files.isric.org/soilgrids/foermer/2017-03-10/data/ (last access: 5 July 2022)	http://54.229.242.119/GSOCmap/ (last access: 5 July 2022)	https://data.dryad.org/stash/data-set/doi:10.7941/D1GD1H (last access: 5 July 2022)
Reference	FAO et al. (2012)	Shangguan et al. (2014)	Batjes. (2016)	Hengl et al. (2017)	FAO and ITPS. (2018)	Mishra et al. (2021)
DOI	NA	https://doi.org/10.1002/2013MS000293	https://doi.org/10.1371/journal.pone.0169748	https://doi.org/10.1016/j.geoderma.2016.01.034	NA	https://doi.org/10.1126/sciadv.aaz5236

115 Notes: NA denotes not available.

2.2 Analysis

To make these datasets comparable, we transformed all datasets to the same coordinate system (WGS1984), calculated SOC density for each layer using the following Eq. (1) and resampled them to a spatial resolution of 30"×30". The transforming, calculating and resampling can be done in ArcGIS10.4 or using open access alternatives (e.g., QGIS, R).

$$120 \quad SOC_D = SOC_C \times BD \times D \times (1 - CF), \quad (1)$$

where SOC_D is SOC density ($t \text{ ha}^{-1}$), SOC_C is SOC content (% weight), BD is soil bulk density ($g \text{ cm}^{-3}$), D is the depth of soil layers (cm), and CF is the coarse fragments (% weight). Due to the different layer schemes of these soil datasets, we figured up SOC density for the depth of 0-30 cm and 0-100 cm by Eq. (2) and (3):

$$SOC_{Di} = \begin{cases} SOC_{Di}, & b \leq m \\ SOC_{Di} \times \frac{m-a}{b-a}, & b > m \end{cases}, (m = 30 \text{ or } 100), \quad (2)$$



$$125 \quad SOC_{D(0-m)} = \sum_{i=1}^n SOC_{Di}, \quad (3)$$

where SOC_{Di} is SOC density ($t \text{ ha}^{-1}$) for each layer, $SOC_{D(0-m)}$ is SOC density ($t \text{ ha}^{-1}$) at 0-30 cm or 0-100 cm depth, m is the target depth (30 cm or 100 cm), a is the upper depth (cm) of layer, b is the bottom depth (cm) of layer, n is the number of soil layers. In each grid, the uncertainty of SOC_D induced by data source (derived from above-mentioned five datasets) is expressed as coefficient of variation for each grid cell by Eq. (4):

$$130 \quad CV = \frac{\sqrt{\frac{1}{N} \sum_{i=1}^N (X_i - \bar{X})^2}}{\bar{X}}, \quad (4)$$

where CV is the coefficient of variation, X_i is SOC density in each dataset, \bar{X} is the average of all soil datasets, N is the total number of the soil datasets.

In the study, soil profiles from the WoSIS were used as a reference to evaluate the uncertainties of the five global soil datasets, and the global land cover data from the MODIS Land Cover Climate Modeling Grid Product (MCD12C1) (Friedl
 135 and Sulla-Menashe, 2015) was used for the evaluation of uncertainties of SOC estimates among biomes. The WoSIS global soil profile database was developed by ISRIC and comprised of a large amount of quality-assessed and standardized soil profiles (about 196498 profiles in the latest version) from 173 countries (Batjes et al., 2020). The MCD12C1 supplied global maps of 17 land cover classes based on the International Geosphere-Biosphere Programme's classification schemes (Friedl and Sulla-Menashe, 2015), and we categorized the global land surfaces into 8 major biomes: forests, shrublands/savannas,
 140 grasslands, croplands, barren lands, urban and built-up lands and permanent wetlands. The lands without soil cover, like water bodies and permanent snow and ice, were not discussed in this study. Here, we represented the comparative results between the WoSIS and other soil datasets using the Taylor diagram, a concise graph that can summarize how closely a model matches the observations. In this diagram, the spatial correlation coefficients and the root mean square errors (RMSE) between simulated and observed fields, as well as the normalized standard deviations of the simulated value from the global mean, can
 145 all be shown by a point in the polar coordinate system (Taylor, 2001, 2005; Hu et al., 2022). The Taylor Diagram can be plotted using MATLAB file from Guillaume (2022) or other open access scripts like R.

3 Results

3.1 Global SOC distribution and stocks

On the global scale, the spatial distributions of 0-30 cm SOC density from the five global datasets are generally consistent,
 150 with values increasing from lower to higher latitudes (Fig. 1 and S1a). Higher SOC density is concentrated in the northern high latitudes including Russia, Northern Europe, Alaska, and northern Canada, along with some equatorial regions between 10° N to 10° S and southern South America. Relatively lower SOC density is found in the mid and low latitudes ranging from 10° N - 50° N and 10° S - 40° S , such as northern and southern Africa, central and western Asia, and Australia. Note that in these



datasets, there are soil information gaps in some areas, including Greenland in the GSOCmap (Fig. 1e), and some regions in
 155 the Sahara Desert in the HWSD (Fig. 1a), WISE30sec (Fig. 1b), and GSDE (Fig. 1c). At the depth of 0-100 cm, the distributions
 of SOC density from the five soil datasets share a consistent pattern with those of 0-30 cm SOC density, with higher values in
 the northern high latitudes and certain equatorial regions (Fig. S1b and S2). For global SOC stocks, the estimates from the five
 soil datasets are in a range of 577-1171 Pg and 1086-2678 Pg with averages of 828 and 1873 Pg, for 0-30 cm 0-100 cm soil
 depths, respectively (Fig. 1f). Among the five datasets, the SOC stocks estimated by the Soilgrids250m is the highest and that
 160 estimated by the HWSD is the lowest. The estimates provided by the WISE30sec and GSDE are relatively comparable.

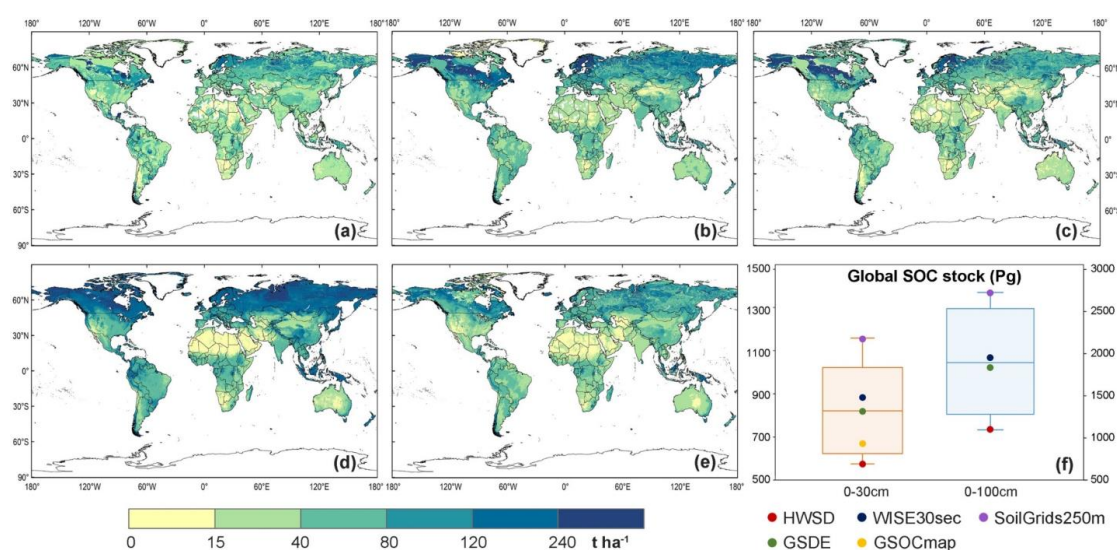


Figure 1: Global SOC density and stocks vary by datasets. (a-e) SOC density of 0-30 cm (t ha^{-1}) based on HWSD, WISE30sec, GSDE, SoilGrids250m, and GSOCmap, respectively. (f) Global SOC stocks (Pg) estimated for five datasets.

3.2 Global SOC density differences among datasets

165 Although the five datasets show similar patterns of SOC density distribution, their magnitudes of SOC density differ globally
 and in specific regions. The coefficient of variations (CV) range from 0.15% to 179% for 0-30 cm SOC density (Fig. 2a) and
 from 0.11% to 163% for 0-100 cm SOC density (Fig. 2b), illustrating the spatial heterogeneity of SOC density among the five
 datasets. The major differences among the five datasets are observed in the northern circumpolar region and the Tibetan Plateau,
 where the most permafrost soils are located. There are also differences in Southeast Asia, some areas of the Sahara Desert, the
 170 basin of the upper White Nile, the Great Basin of Australia and some valleys around the Cordillera. Meanwhile, in these regions,
 the five datasets differ more at 0-100 cm depth than at 0-30 cm depth.

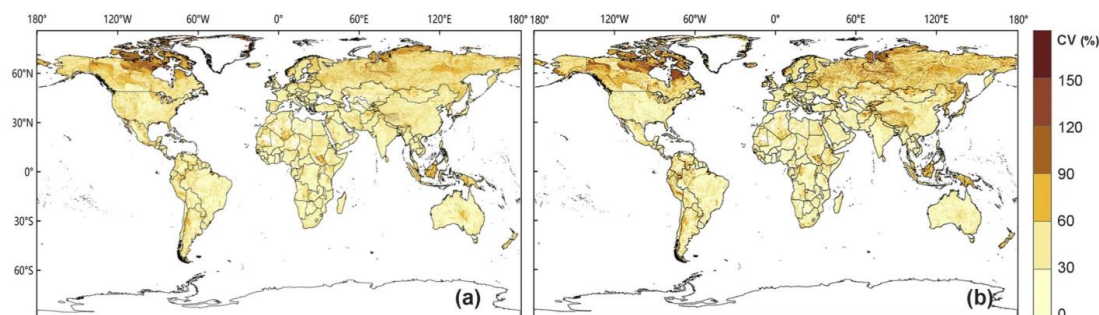


Figure 2: The coefficient of variations (CV, %) estimated for (a) 0-30 cm and (b) 0-100 cm SOC density (t ha^{-1}) using five datasets.

The differences among datasets can be further evidenced by using the mean of the five datasets as the benchmark.

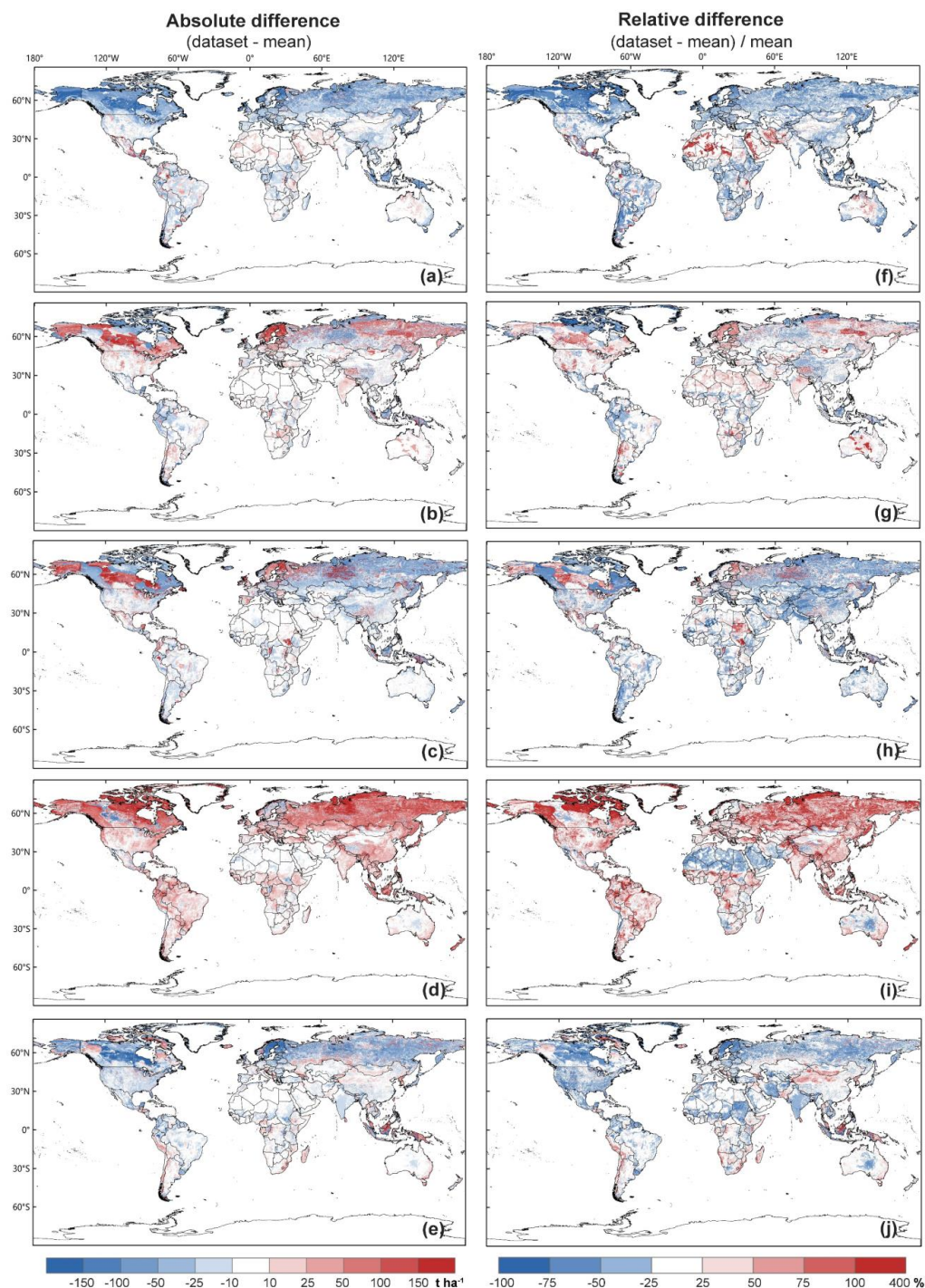
175 Generally, for 0-30 cm SOC density, the HWSD has negative biases (Fig. 3a) and the SoilGrids250m has positive biases (Fig. 3d). The WISE30sec, GSDE and GSOCmap are relatively close to the mean in the spatial distribution of SOC density (Fig. 3b, 3c and 3e). Specifically, in the northern circumpolar region, where the differences are significant, the WISE30sec and SoilGrids250m have positive deviations from the mean, while the HWSD, GSDE and GSOCmap have negative deviations. The magnitude of SOC density estimated by the SoilGrids250m is the highest in most areas of world, followed by the

180 WISE30sec, GSDE and GSOCmap, and that estimated by the HWSD is the lowest (Fig. S3). However, in Northern Europe and Northwest Canada, the SoilGrids250m is 100 t ha^{-1} lower at least than the WISE30sec and GSDE, while it is higher than the HWSD and GSOCmap (Fig. S3). In Southeast Asia, the biases of the SoilGrids250m and the GSOCmap from the mean are positive, while those of the HWSD, WISE30sec and GSDE are negative. The SOC density estimate of the SoilGrids250m is $50\text{-}300 \text{ t ha}^{-1}$ larger than that of the GSOCmap, and the estimates of the WISE30sec and GSDE are similar, both higher than

185 that of the HWSD (Fig. S3).

Furthermore, the relative differences between the individual dataset and the mean magnify the details of discrepancy among the datasets on the regional scale (Fig. 3f-j). In the parts of northern Africa and the Middle East, the HWSD is above the mean and the SoilGrids250m is below the mean, opposite to the biases in other regions. In central Australia, the HWSD and WISE30sec have positive deviations from the mean and others have negative deviations, but the differences across the

190 five datasets are relatively small (within approximately $\pm 50 \text{ t ha}^{-1}$) (Fig. S3). In the basin of the upper White Nile, the SOC density estimated by the GSDE is over 300 t ha^{-1} higher than that estimated by others (Fig. S3). For 0-100 cm SOC density estimates, the pattern of differences among the soil datasets is similar with that at 0-30 cm depth, but the magnitude of biases is larger (Fig. S4).



195 **Figure 3:** Differences of 0-30cm SOC density (t ha^{-1}) between individual dataset and the mean. The mean is the average of the five datasets. Left column is the absolute difference of (a) HWSD, (b) WISE30sec, (c) GSDE, (d) SoilGrids250m, and (e) GSOCmap. Right column is the relative difference of (f) HWSD, (g) WISE30sec, (h) GSDE, (i) SoilGrids250m, and (j) GSOCmap.



In comparison with WoSIS reference, the five soil datasets generally provide a better estimate of SOC density for 0-30 cm depth than for 0-100 cm depth. The correlation coefficients of five datasets with the WoSIS range from 0.19 to 0.47 for 0-30 cm (Fig. 4a) and from 0.14 to 0.48 for 0-100 cm (Fig. 4b). The root mean square errors (RMSE) for 0-30 cm SOC density is at the range of 0.94 to 1.28 (Fig. 4a), which is slightly smaller than that for 0-100 cm (0.98-1.48) (Fig. 4b). The normalized standard deviation of 0-30 cm SOC density is from 0.56 to 1.03 (Fig. 4a) and that of 0-100 cm is from 0.50 to 1.23 (Fig. 4b). The SOC density simulations from the SoilGrids250m are the closest to the observations from the WoSIS at both 0-30 cm and 0-100 cm depths (the correlation coefficients are 0.47 and 0.48, respectively). At 0-30 cm depth, the simulations from the GSOCmap are also relatively close to the WoSIS (the correlation coefficient is 0.31). The HWSD, WISE30sec and GSDE are weakly correlated with the WoSIS, and it is related to the different metadata sources of these soil datasets (Fig. 9). The amplitudes of the WISE30sec and GSDE are similar to the WoSIS at 0-30 cm depth. The lower standard deviation of the HWSD indicates that there is an underestimation of SOC density in the local region of the HWSD compared to the WoSIS.

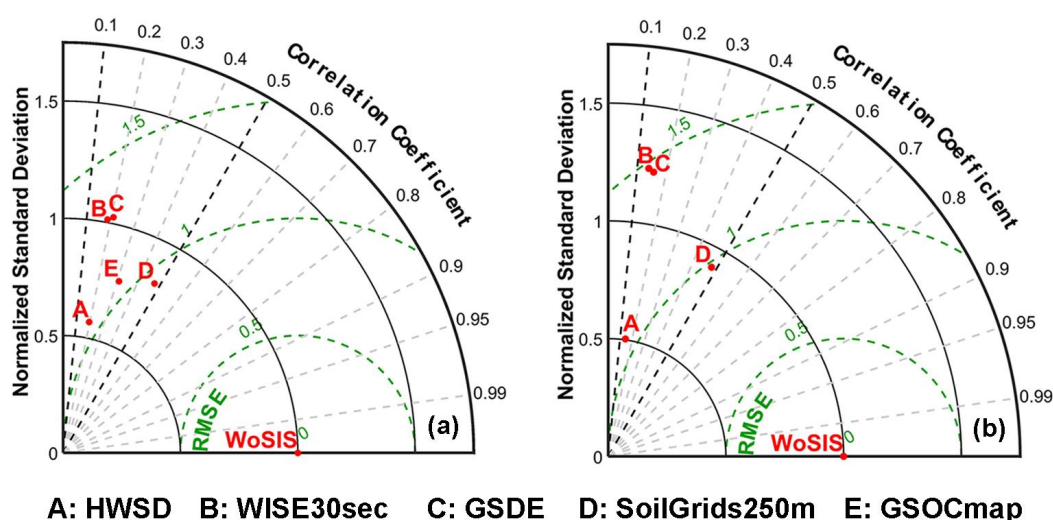


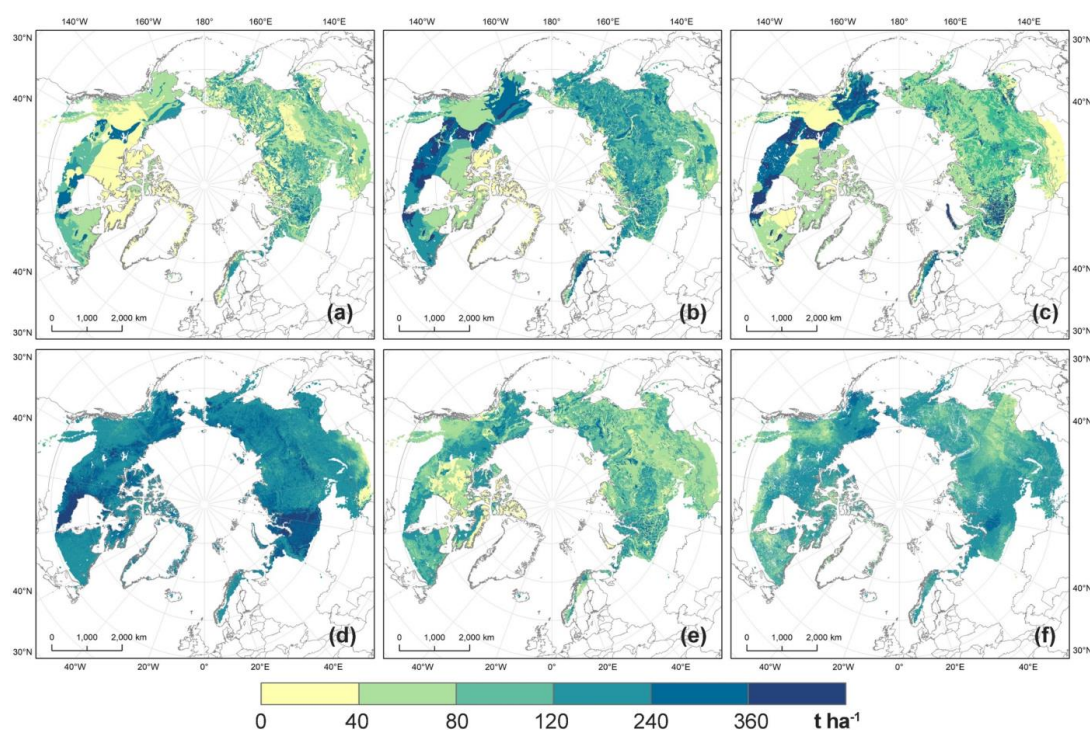
Figure 4: Normalized Taylor diagram of the comparison of SOC density (t ha^{-1}) between WoSIS and individual soil dataset at the depth of (a) 0-30 cm ($n=14771$) and (b) 0-100 cm ($n=15245$). The GSOCmap only includes 0-30 cm SOC density estimates.

3.3 Regional SOC density differences among datasets

The largest discrepancy among the global soil datasets is found in the northern circumpolar region and the Tibetan Plateau, where most permafrost-affected soils are located (Fig. 2). The UM2021, the regional permafrost dataset reported by Mishra et al., (2021), is used to compare the simulations and uncertainties of the SOC density in these areas. In the northern circumpolar permafrost region, the high simulations of 0-30 cm SOC density are concentrated in West Siberian Plain, Alaska, and from Northwest Territories to the southern shore of Hudson Bay in Canada (Fig. 5), where the Histosol and Gleysol are widely located. Overall, the SoilGrids250m presented the highest SOC density, followed by WISE30sec, UM2021 and GSDE. The



GSOCmap lacks soil information for Greenland Island, and its estimated SOC density is relatively higher than HWSD and
 220 lower than GSDE. Compared with the mean of the six datasets, the SOC density estimated by UM2021 is the closest, followed
 by the WISE30sec, GSDE and GSOCmap, and the SoilGrids250m and HWSD have the largest positive and negative deviation,
 respectively (Fig. S5). The CVs show the differences across the datasets in the northern circumpolar permafrost region are
 distributed in northern Canada (60° - 80° N, 60° - 120° W), the basins of Ob River and Yenisei River on the Western Siberian
 Plain (60° - 75° N, 60° - 90° E) (Fig. S6a). Specifically, in northern Canada, SOC density estimated by the SoilGrids250m and
 225 UM2021 are above the mean and the deviation of SoilGrids250m is larger than that of UM2021 (Fig. S5). In the Western
 Siberian Plain, the discrepancy across the five datasets is mainly due to the high SOC density of SoilGrids250m which is
 overall higher than the mean ($>200 \text{ t ha}^{-1}$) (Fig. S5). Differences among the soil datasets for 0-100 cm SOC estimates are more
 extensive for 0-30 cm SOC estimates, although their distribution patterns are similar (Fig. S6b, S7 and S8).



230 **Figure 5: Spatial distribution of 0-30 cm SOC density (t ha^{-1}) in the northern circumpolar permafrost region from (a)HWSD, (b)WISE30sec, (c)GSDE, (d)SoilGrids250m, (e)GSOCmap and (f) UM2021.**

In the Tibetan Plateau, the estimated 0-30 cm SOC of most datasets decreases gradually from southeast to northwest (Fig.
 6a and c-f), except WISE30sec (Fig. 6b). Relatively, the SOC density simulated by GSDE, SoilGrids250m and UM2021 are
 closer to the pattern of SOC distribution based on the Tibetan Plateau observations, with high values in the forest of
 235 southeastern Tibetan Plateau and low values in the desert of northwestern Tibetan Plateau (Wang et al., 2019; Tian et al., 2008).



The large CVs among the datasets are found in the western and southeastern Tibetan Plateau, as well as the Tsaidam Basin (Fig. S9a). Compared with the mean of the six datasets, the SoilGrids250m and UM2021 has the largest positive and negative overall deviation, respectively. However, the SoilGrids250m is lower than the mean in the western Tibetan Plateau and the Tsaidam Basin, and the UM2021 is higher than the mean in the southeastern Tibetan Plateau (Fig. S10). The SOC density simulated by HWSD and GSOCmap are relatively close to the mean in the western Tibetan Plateau and higher than the mean in the Tsaidam Basin (Fig. S10). Different from the SOC distribution patterns of other datasets, the SOC density estimated by the WISE30sec is higher than the mean in the western Tibetan Plateau, which results in the large CVs of this region (Fig. S10). For 0-100 cm SOC estimates, the differences across soil datasets are more significant for 0-30 cm SOC estimates, although their distribution patterns are comparable (Fig. S9b, S11 and S12).

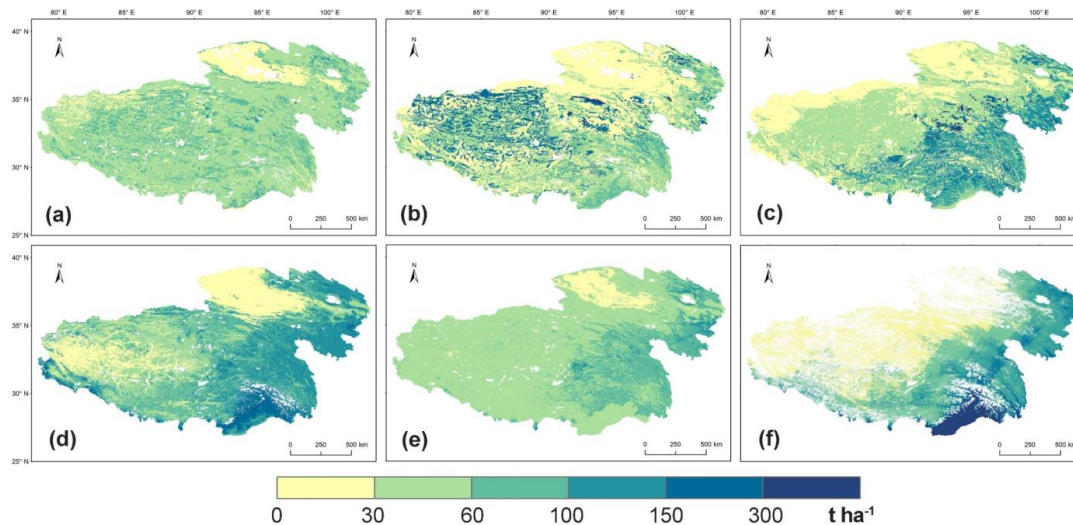


Figure 6: Spatial distribution of 0-30 cm SOC density (t ha^{-1}) in the Tibetan permafrost region from (a)HWSD, (b)WISE30sec, (c)GSDE, (d)SoilGrids250m and (e)UM2021, (f)GSOCmap and (f) UM2021.

3.4 SOC estimates by biomes

The Taylor diagrams indicate that the five soil datasets perform relatively better in estimating SOC density of grasslands, croplands and shrublands/savannas than other biomes, with correlation coefficients ranging from 0.1-0.6 and normalized standard deviations of approximately 1.0 (Fig. 7). The performance is poor in the simulation of SOC density in permanent wetlands, with correlation coefficients ranging from -0.2 to 0.5 and normalized standard deviations over 2.0 (Fig. 7). For SOC estimates over forests, normalized standard deviations are below 1.0 for all five datasets, indicating that the SOC estimates from five datasets are lower than the WoSIS observations in this biome (Fig. 7). The poor performance of permanent wetlands and forests may relate to the low sampling density of these biomes (Fig. S13). For SOC estimates in different biomes, the five global soil datasets have different performances. The SoilGrids250m shows the closest correlation to the WoSIS observations



for SOC estimates in most biomes, followed by GSOCmap, and HWSD underperforms all other datasets in most biomes (Fig. 7). In croplands and urban and built-up lands, SoilGrids250m has larger normalized standard deviations with WoSIS (0.5 of croplands and 1.5 of urban and built-up lands, respectively), though it is still closer to WoSIS than others (Fig. 7). Compared with SOC estimates of other biomes, the WISE30sec performs better in shrublands/savannas and urban and built-up lands, and GSDE performs better in croplands (Fig. 7).

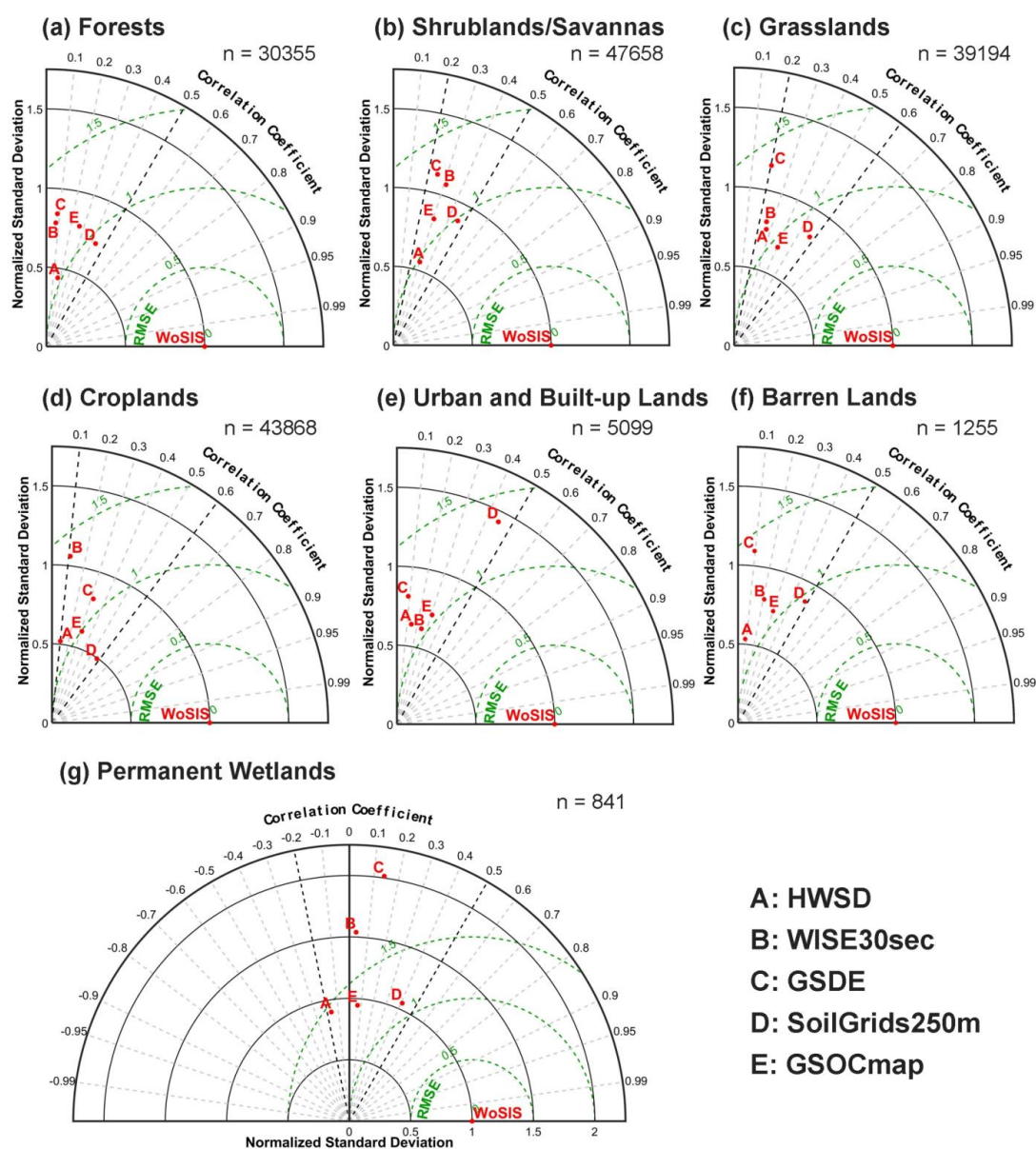


Figure 7: Normalized Taylor diagrams of the comparison of 0–30 cm SOC density (t ha^{-1}) between WoSIS and individual soil dataset for different biomes. N is the number of WoSIS soil profiles in each biome.



265 4 Discussion

4.1 Overall assessment of SOC estimates

In this study, the results indicate no consensus on global SOC estimates in these observation-based estimates, and each dataset performs differently in specific regions. Generally, in terms of both simulation quality and sampling density, the GSOCmap provides preferable global SOC estimates at 0-30 cm depth, while the SoilGrids250m and GSDE simulate the global SOC magnitudes and distribution better at both 0-30 cm and 0-100 cm depth (Fig. 8). In the northern circumpolar permafrost region, the UM2021 has the smallest uncertainty on SOC simulations, followed by the WISE30sec. In China, the GSDE offers the best SOC estimation using a large amount of soil observational data, particularly in the Tibetan Plateau. As shown in Fig. 8, for specific regions, the size of the circles indicates the discrepancies among these estimates. The larger the circle, the greater the differences in the data quality or sampling density in this area for the datasets involved in the comparison. For instance, in the northern circumpolar permafrost region (region 4 in Fig. 8), the soil sampling density is much lower than in other regions due to the variation in the extent of the permafrost region and the harsh climatic conditions, which affects the prediction of the SOC spatial heterogeneity and the uncertainty of measurements (Köchy et al., 2015a; Mishra et al., 2013, 2021). In China (region 1 in Fig. 8) and Africa (region 6 in Fig. 8), the differences among the five datasets are relatively smaller in data quality and sampling density dimensions, while the variability in Southeast Asia (region 2 in Fig. 8) is larger. Compared with other datasets, the SoilGrids250m has greater SOC estimates in most high latitudes and some tropical islands, like Sri Lanka (Vitharana et al., 2019), though it is very close to the observations from the WoSIS. However, these datasets have advantages and limitations in different aspects of simulation. For example, the GSDE has most abundant soil information, with 34 soil properties up to 2.3 m depth, which can satisfy the diversity of applications (e.g., modeling). The GSOCmap specifically targets at 0-30 cm SOC data, without capability to reflect more soil properties and soil carbon information at variable depth intervals (Table S1).

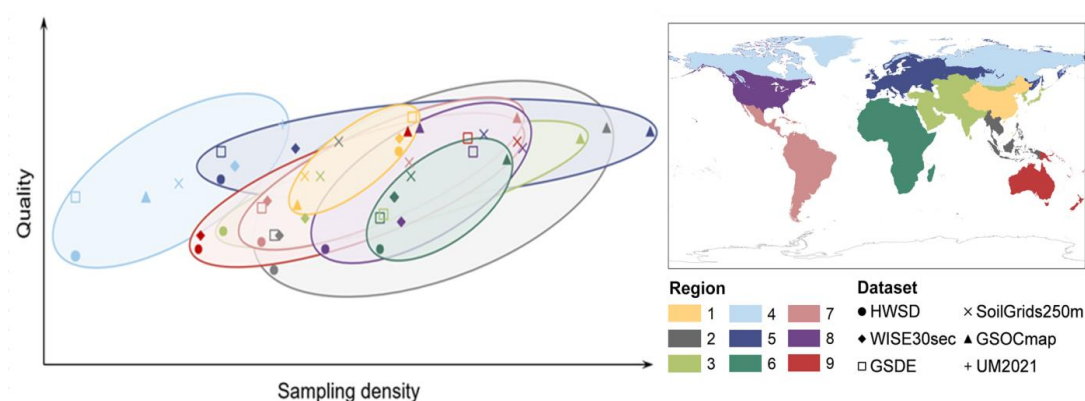


Figure 8: A qualitative assessment of soil datasets at the regional scale. The circles with different colors represent different regions.



4.2 Sources of differences and future needs

The diversity of data sources and different mapping methods are important reasons for the differences among soil datasets. The
290 conventional mapping approach is the knowledge-based linkage method (also known as the taxotransfer rule-based method),
which links soil profiles and soil mapping units on soil type maps (Batjes, 2003; Dai et al., 2019). The HWSD, GSDE, and
WISE30sec are constructed using this approach, and the field observations these estimates used are more or less related (Fig.
9a). In recent decades, the digital soil mapping methods have been used to generate SOC estimates, and it is modeled using
machine learning or other spatial interpolation approaches based on soil profiles and environmental covariates such as climate,
295 topography, and land use (McBratney et al., 2003; Hengl et al., 2017). The SoilGrids250m and GSOCmap both use digital soil
mapping methods, and their data sources are also somewhat similar (Fig. 9b). The SOC estimates generated by digital mapping
methods usually better reflect continuous spatial variation in soil properties than those using the linkage methods. Adjacent soil
types in reality often have no obvious spatial boundaries, but rather there is a certain range of transition zones, and the soil
properties in the transition zones are similar to the adjacent soils. However, the linkage method assigns only one statistical
300 value to the soil type in the soil unit, resulting in abrupt changes in attribute values at the boundaries of the soil polygon (Dai
et al., 2019; Zhu et al., 2018). Moreover, the quality of field observations impacts the robustness of generated SOC estimates.
For instance, the parts of the HWSD that still utilizes the DSMW such as North America, Australia, West Africa (excluding
Senegal and Gambia) and South Asia are considered less reliable, while most of the areas covered by SOTWIS databases are
considered to have higher reliability (FAO et al., 2012) (Fig. S14).

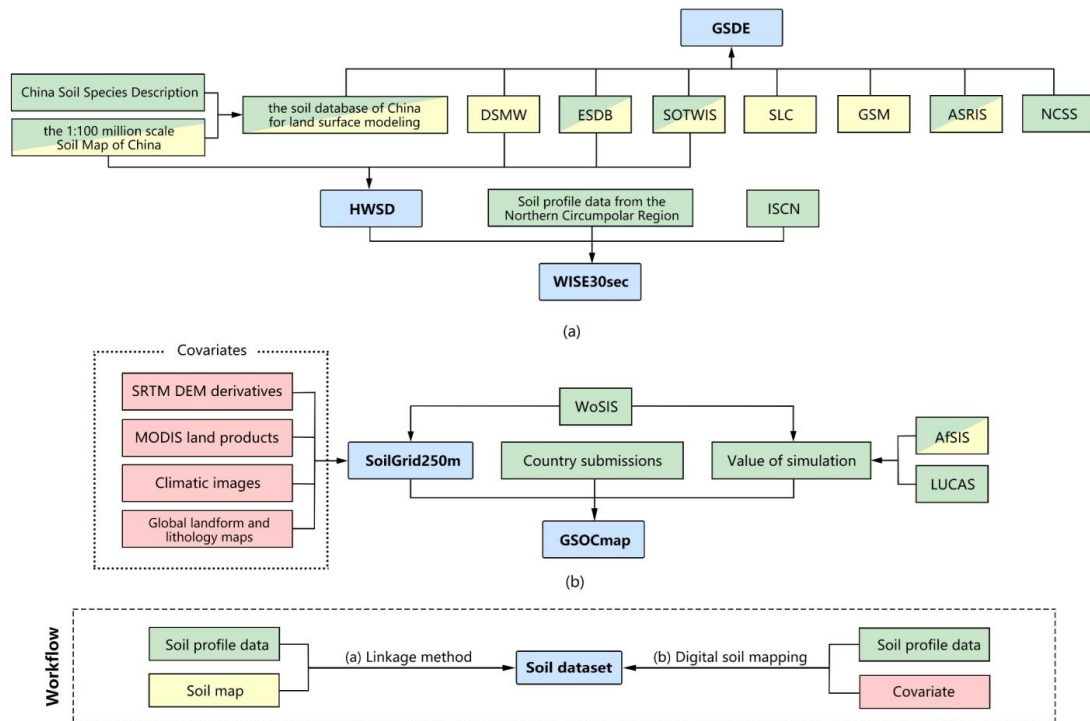


Figure 9: Data sources of global soil datasets. The sources include DSMW (the Digital Soil Map of the World), ESDB (the European Soil Database), SOTWIS (SOTER and WISE-derived databases), ISCN (International Soil Carbon Network), SLC (the Soil Landscapes of Canada), GSM (the U.S. General Soil Map), ASRIS (the Australian Soil Resource Information System polygon attributed surface), NCSS (National Cooperative Soil Characterization Database), WoSIS (the World Soil Information Service soil profile database), AfSIS (Africa Soil Information Service), LUCAS (Land Use and Coverage Area frame Survey).

In addition to the objective disparities among SOC estimates, the different estimation approaches also contribute to diverse estimates of SOC stocks (Table. 2). For example, Köchy et al. (2015a) and Tifafi et al. (2018) calculated widely varying global SOC stocks at 0–100 cm depth, although their estimates were based on the same dataset. Since SOC estimates are dependent on numerous factors such as SOC content, bulk density, and coarse fragments, uncertainty and/or errors in measurement of one factor may affect the final SOC stock estimation (Köchy et al., 2015a; Poeplau et al., 2017). In the estimate from Hiederer and Köchy (2011), notable differences in global SOC stock estimates were ascribed to the varying bulk density parameters.



Table 2 Different estimates for SOC stocks at the depth of 0-100 cm and 0-30 cm

Depth (cm)	SOC stock (Pg C)	Data source	Reference
0-100	2500	HWSD v1.2	(Tifafi et al., 2018)
	3400	SoilGrids250m v1.0	(Tifafi et al., 2018)
	1325	HWSD v1.2	(Köchy et al., 2015a)
	1408±154	WISE30sec	(Batjes, 2015)
	504-3000	27 datasets	(Scharlemann et al., 2014)
	1417	HWSD v1.1	(Hiederer and Köchy, 2011)
	1399	NRCS	(Hiederer and Köchy, 2011)
	1459	FAO2007	(Hiederer and Köchy, 2011)
	991	WISE5by5min	(Hiederer and Köchy, 2011)
	1206	DSMW	(Hiederer and Köchy, 2011)
	1500	16 estimates	(Amundson, 2001)
0-30	1462-1548	WISE	(Batjes, 1996)
	680	GSOCmap v1.5	(FAO and ITPS, 2018)
	1267	SoilGrids250m	(FAO and ITPS, 2018)
	755±119	WISE30sec	(Batjes, 2015)
	699	HWSD V1.1	(Hiederer and Köchy, 2011)
	504	WISE5by5min	(Hiederer and Köchy, 2011)
	574	DSMW	(Hiederer and Köchy, 2011)
	684-724	WISE	(Batjes, 1996)

320 To further improve the overall accuracy of soil data, future work is expected to narrow the circles in Figure 8 and bring them closer to the upper right corner. First of all, it is essential to establish a unified and standardized system for soil sampling, measurement, recording and calculation methods in the global SOC simulation, which requires global soil science communities to collaborate and work collectively (Onerhime, 2021). Secondly, data sources need to be populated with all possible efforts to appropriately cover different regions and biomes (Fig. 8 and S13). The potential solutions can be region-specific and biome-specific. For example, in the Northern circumpolar region (Fig. 8), or for forest and wetlands (Fig. S13), the sampling density of soil profiles could be increased, and soil profile data sharing among the various soil databases should be promoted given the inherent difficulties of sampling and measuring in this region (Mishra et al., 2013). In the regions (e.g., China, and North America) (Fig. 8) or biomes (e.g., croplands) (Fig. S13) with higher density of observations, soil datasets can be summarized and integrated to form a more accurate database. In the regions with large differences among field observations, using more reliable data sources and enhancing soil sampling campaigns are necessary to reduce the uncertainty in SOC estimation. Last



but not the least, data sharing should be further encouraged along the line of dataset development, e.g., during planning, sampling, measuring, cross-validation, mapping at either individual, regional or national level (Lobry de Bruyn and Ingram, 2019). Citizen science, and cross-program (programs with needs for soil sampling) collaborations should also be pursued as options for soil data collection (Rossiter et al., 2015; Robinson et al., 2019).

335 5 Conclusions

Global SOC density and stocks vary greatly among different datasets. The overall stocks are at a range of 577-1171 Pg and 1086-2678 Pg with averages of 828 and 1873 Pg, for 0-30 cm 0-100 cm soil depths, respectively. In terms of spatial distribution, the SOC density is higher in the high latitudes and equatorial regions, and the SOC density gradually increases from low latitude to high latitude. Globally, GSOCmap provides relatively accurate estimate of SOC stocks at 0-30 cm depth, and SoilGrids250m
 340 and GSDE perform better for simulations at multiple depths. At the regional scale, these five SOC estimates have various accuracies in different areas, and the largest differences are in the northern circumpolar and Tibetan Plateau permafrost regions. The UM2021 and WISE30sec perform better in the northern circumpolar permafrost regions, and GSDE performs better in China. For different biomes, the five soil datasets show better performance in simulating SOC density of grasslands, croplands and shrublands/savannas, and perform poorly over permanent wetlands. The uncertainty in SOC estimates mainly comes from
 345 soil sampling density, diverse sources and mapping methods, as well as the interpolation methods used by different authors. In the future, to reduce the uncertainty in SOC estimates, the sample density of soil profiles should be increased in areas and biomes with large SOC uncertainties, and global cooperation and data sharing should be further encouraged.

Data availability

We made all the data used in this study publicly accessible to assist reduce the uncertainty in global and regional SOC estimates.
 350 This dataset includes 7 TIFF files for 0-30 cm SOC density from the five global soil datasets and the regional permafrost dataset (spatial resolution: 30", units: t ha⁻¹) and 6 TIFF files for 0-100 cm SOC density from the four global soil datasets and the regional permafrost dataset (spatial resolution: 30", units: t ha⁻¹). The free availability of this dataset does not imply free publication. Any use of this dataset should include appropriate acknowledgement to the original data sources. This dataset is available at <https://doi.org/10.6084/m9.figshare.20220234> (Lin et al., 2022). The information provided in Table S2 lists links
 355 for downloading global and regional datasets used in this study.

Supplement.

The supplement related to this article is available online at: ...



Author contributions.

Z. Q. conceived the idea and designed the study. Z. L. and Z. Q. collected and analyzed the datasets, and Y. D., U. M., G. W., W.
 360 Z., and W. S. helped with interpretation of the results. Y. D. and W. S. provided help with GSDE dataset, U. M. helped with
 UM2021 data access. Z. L. and Z. Q. wrote the main manuscript with contributions from all authors. All authors reviewed and
 edited the manuscript.

Competing interests.

The authors declare that they have no conflict of interests.

365 Acknowledgements.

We are very grateful to Dr. Giulio Genova for communicating on soil product use of SoilGrid250m, and other authors and
 developers of the global and regional soil datasets for sharing their knowledge and products.

Financial support.

This work has been partially supported by the National Natural Science Foundation of China (U21A6001, 41975113), and the
 370 Guangdong Provincial Department of Science and Technology (2019ZT08G090).

References

- Amundson, R.: The Carbon Budget in Soils, *Annu. Rev. Earth Planet. Sci.*, 29, 535–562,
<https://doi.org/10.1146/annurev.earth.29.1.535>, 2001.
- Bastida, F., García, C., Fierer, N., Eldridge, D. J., Bowker, M. A., Abades, S., Alfaro, F. D., Asefaw Berhe, A., Cutler, N. A.,
 375 Gallardo, A., García-Velázquez, L., Hart, S. C., Hayes, P. E., Hernández, T., Hseu, Z.-Y., Jehmlich, N., Kirchmair, M.,
 Lambers, H., Neuhauser, S., Peña-Ramírez, V. M., Pérez, C. A., Reed, S. C., Santos, F., Siebe, C., Sullivan, B. W., Trivedi,
 P., Vera, A., Williams, M. A., Luis Moreno, J., and Delgado-Baquerizo, M.: Global ecological predictors of the soil priming
 effect, *Nat. Commun.*, 10, 3481, <https://doi.org/10.1038/s41467-019-11472-7>, 2019.
- Batjes, N. H.: Total carbon and nitrogen in the soils of the world, *European Journal of Soil Science*, 47, 151–163,
 380 <https://doi.org/10.1111/j.1365-2389.1996.tb01386.x>, 1996.
- Batjes, N. H.: A taxotransfer rule-based approach for filling gaps in measured soil data in primary SOTER databases (version.
 1.1), ISRIC – World Soil Information, Wageningen, the Netherlands, ISRIC Report 2003/03, 44 pp, 2003.



- Batjes, N. H.: ISRIC-WISE global data set of derived soil properties on a 0.5 by 0.5 degree grid (Version 3.0), ISRIC – World Soil Information, Wageningen, the Netherlands, ISRIC Report 2005/08, 20 pp, 2005.
- 385 Batjes, N. H.: ISRIC-WISE derived soil properties on a 5 by 5 arc-minutes global grid (ver.1.2), ISRIC – World Soil Information, Wageningen, the Netherlands, ISRIC Report 2012/01, 52 pp, 2012.
- Batjes, N. H.: World soil property estimates for broad-scale modelling (WISE30sec), ISRIC – World Soil Information, Wageningen, the Netherlands, ISRIC Report 2015/01, 68 pp, 2015.
- Batjes, N. H.: Harmonized soil property values for broad-scale modelling (WISE30sec) with estimates of global soil carbon
 390 stocks, *Geoderma*, 269, 61–68, <https://doi.org/10.1016/j.geoderma.2016.01.034>, 2016.
- Batjes, N. H. and Gicheru, P.: Soil data derived from SOTER for studies of carbon stocks and change in Kenya (version. 1.0), ISRIC – World Soil Information, Wageningen, the Netherlands, ISRIC Report 2004/01, 37 pp, 2004.
- Batjes, N. H., Rawajfih, Z., and Al-Adam, R.: Soil data derived from SOTER for studies of carbon stocks and change in Jordan (version 1.0), ISRIC – World Soil Information, Wageningen, the Netherlands, ISRIC Report 2003/04, 34 pp, 2003.
- 395 Batjes, N. H., Bhattacharyya, T., Mandal, C., Dijkshoorn, K., Pal, D. K., Milne, E., and Gajbhiye, K. S.: Soil data derived from SOTER for studies of carbon stocks and change in the Indo-Gangetic Plains (India) (version 1.0), ISRIC – World Soil Information, Wageningen, the Netherlands, ISRIC Report 2004/06, 37 pp, 2004.
- Batjes, N. H., Ribeiro, E., van Oostrum, A., Leenaars, J., Hengl, T., and Mendes de Jesus, J.: WoSIS: providing standardised soil profile data for the world, *Earth Syst. Sci. Data*, 9, 1–14, <https://doi.org/10.5194/essd-9-1-2017>, 2017.
- 400 Batjes, N. H., Ribeiro, E., and van Oostrum, A.: Standardised soil profile data to support global mapping and modelling (WoSIS snapshot 2019), *Earth Syst. Sci. Data*, 12, 299–320, <https://doi.org/10.5194/essd-12-299-2020>, 2020.
- Ciais, P., Sabine, C., Bala, G., Bopp, L., Brovkin, V., Canadell, J., Chhabra, A., DeFries, R., Galloway, J., Heimann, M., Jones, C., Quéré, C. L., Myneni, R. B., Piao, S., and Thornton, P.: Anthropogenic and Natural Radiative Forcing, in: *Climate Change 2013 – The Physical Science Basis: Working Group I Contribution to the Fifth Assessment Report of the Intergovernmental Panel on Climate Change*, Cambridge University Press, Cambridge, 659–740, <https://doi.org/10.1017/CBO9781107415324.018>, 2013.
- 405 Dai, Y., Shangguan, W., Wei, N., Xin, Q., Yuan, H., Zhang, S., Liu, S., Lu, X., Wang, D., and Yan, F.: A review of the global soil property maps for Earth system models, *SOIL*, 5, 137–158, <https://doi.org/10.5194/soil-5-137-2019>, 2019.
- van Engelen, V. W. P. and Dijkshoorn, J. A.: Global and National Soils and Terrain Databases (SOTER), ISRIC – World Soil
 410 Information, Wageningen, the Netherlands, ISRIC Report 2013/04, 198 pp, 2013.
- van Engelen, V. W. P., Batjes, N. H., Dijkshoorn, J. A., and Huting, J. R. M.: Harmonized Global Soil Resources Database, ISRIC – World Soil Information and FAO, ISRIC Report 2005/06, 17 pp, 2005.



- FAO: FAO- Unesco Soil map of the world (1: 5000000), FAO/UNESCO [data set], 1974.
- FAO: FAO-Unesco Soil map of the world (revised legend, with corrections and updates), FAO, Rome, Italy, World Soil
 415 Resources Report 60, 146 pp, 1988.
- FAO: Digitized Soil Map of the World and Derived Soil Properties, FAO/UNESCO [data set], 1995.
- FAO and ITPS: Global Soil Organic Carbon Map (GSOCmap) Technical Report, FAO, Rome, Italy, 162, 2018.
- FAO, IIASA, ISRIC, ISSCAS, and JRC: Harmonized World Soil Database (version 1.2), FAO and IIASA [data set], 2012.
- Friedl, M. A. and Sulla-Menashe, D.: MCD12C1 MODIS/Terra+Aqua Land Cover Type Yearly L3 Global 0.05Deg CMG V006,
 420 NASA EOSDIS Land Processes DAAC [data set], <https://doi.org/10.17040/ISCN/1305039>, 2015.
- Guillaume, M.: Taylor Diagram, MATLAB Central File Exchange [code],
<https://www.mathworks.com/matlabcentral/fileexchange/20559-taylor-diagram>, 2022.
- Hengl, T., de Jesus, J. M., MacMillan, R. A., Batjes, N. H., Heuvelink, G. B. M., Ribeiro, E., Samuel-Rosa, A., Kempen, B.,
 Leenaars, J. G. B., Walsh, M. G., and Gonzalez, M. R.: SoilGrids1km — Global Soil Information Based on Automated
 425 Mapping, PLoS ONE, 9, e105992, <https://doi.org/10.1371/journal.pone.0105992>, 2014.
- Hengl, T., de Jesus, J. M., Heuvelink, G. B. M., Ruiperez Gonzalez, M., Kilibarda, M., Blagotić, A., Shangguan, W., Wright,
 M. N., Geng, X., Bauer-Marschallinger, B., Guevara, M. A., Vargas, R., MacMillan, R. A., Batjes, N. H., Leenaars, J. G.
 B., Ribeiro, E., Wheeler, I., Mantel, S., and Kempen, B.: SoilGrids250m: Global gridded soil information based on machine
 learning, PLoS ONE, 12, e0169748, <https://doi.org/10.1371/journal.pone.0169748>, 2017.
- 430 Hiederer, R. and Köchy, M.: Global soil organic carbon estimates and the harmonized world soil database, European
 Commission Joint Research Centre Institute for Environment and Sustainability, 79 pp, 2011.
- Houghton, R. A.: Balancing the Global Carbon Budget, Annu. Rev. Earth Planet. Sci., 35, 313–347,
<https://doi.org/10.1146/annurev.earth.35.031306.140057>, 2007.
- Hu, Q., Li, T., Deng, X., Wu, T., Zhai, P., Huang, D., Fan, X., Zhu, Y., Lin, Y., Xiao, X., Chen, X., Zhao, X., Wang, L., and Qin,
 435 Z.: Intercomparison of global terrestrial carbon fluxes estimated by MODIS and Earth system models, Science of The Total
 Environment, 810, 152231, <https://doi.org/10.1016/j.scitotenv.2021.152231>, 2022.
- Köchy, M., Hiederer, R., and Freibauer, A.: Global distribution of soil organic carbon – Part 1: Masses and frequency
 distributions of SOC stocks for the tropics, permafrost regions, wetlands, and the world, SOIL, 1, 351–365,
<https://doi.org/10.5194/soil-1-351-2015>, 2015a.
- 440 Köchy, M., Don, A., van der Molen, M. K., and Freibauer, A.: Global distribution of soil organic carbon – Part 2: Certainty of
 changes related to land use and climate, SOIL, 1, 367–380, <https://doi.org/10.5194/soil-1-367-2015>, 2015b.
- Lal, R.: Soil Carbon Sequestration Impacts on Global Climate Change and Food Security, Science, 304, 1623–1627,



- <https://doi.org/10.1126/science.1097396>, 2004.
- Leenaars, J. G. B., van Oostrum, A. J. M., and Ruiperez Gonzalez, M.: Africa Soil Profiles Database Version 1.2. A compilation
 445 of georeferenced and standardised legacy soil profile data for Sub-Saharan Africa (with dataset), Africa Soil Information
 Service (AfSIS) project and ISRIC - World Soil Information, ISRIC Report 2014/01, 166 pp, 2014.
- Lin, Z., Dai, Y., Mishra, U., Wang, G., Zhang, W., Shangguan, W., and Qin, Z.: Global SOC datasets for 0-30 cm and 0-100 cm
 depths, <https://doi.org/10.6084/m9.figshare.20220234>, 2022.
- Lobry de Bruyn, L. and Ingram, J.: Soil information sharing and knowledge building for sustainable soil use and management:
 450 insights and implications for the 21st Century, *Soil Use and Management*, 35, 1–5, <https://doi.org/10.1111/sum.12493>,
 2019.
- Lorenz, K. and Lal, R.: Soil Organic Carbon Sequestration, in: *Soil Organic Carbon Sequestration in Terrestrial Biomes of the
 United States*, edited by: Lorenz, K. and Lal, R., Springer International Publishing, Cham, 55–145,
https://doi.org/10.1007/978-3-030-95193-1_3, 2022.
- 455 McBratney, A. B., Mendonça Santos, M. L., and Minasny, B.: On digital soil mapping, *Geoderma*, 117, 3–52,
[https://doi.org/10.1016/S0016-7061\(03\)00223-4](https://doi.org/10.1016/S0016-7061(03)00223-4), 2003.
- McKenzie, N. J., Jacquier, D. W., Ashton, L. J., and Cresswell, H. P.: Estimation of Soil Properties Using the Atlas of Australian
 Soils, CSIRO Land and Water, Technical Report 11/00, 24 pp, 2000.
- Mishra, U., Jastrow, J. D., Matamala, R., Hugelius, G., Koven, C. D., Harden, J. W., Ping, C. L., Michaelson, G. J., Fan, Z.,
 460 Miller, R. M., McGuire, A. D., Tamocai, C., Kuhry, P., Riley, W. J., Schaefer, K., Schuur, E. A. G., Jorgenson, M. T., and
 Hinzman, L. D.: Empirical estimates to reduce modeling uncertainties of soil organic carbon in permafrost regions: a
 review of recent progress and remaining challenges, *Environ. Res. Lett.*, 8, 035020, <https://doi.org/10.1088/1748-9326/8/3/035020>, 2013.
- Mishra, U., Hugelius, G., Shelef, E., Yang, Y., Strauss, J., Lupachev, A., Harden, J. W., Jastrow, J. D., Ping, C.-L., Riley, W. J.,
 465 Schuur, E. A. G., Matamala, R., Siewert, M., Nave, L. E., Koven, C. D., Fuchs, M., Palmtag, J., Kuhry, P., Treat, C. C.,
 Zubrzycki, S., Hoffman, F. M., Elberling, B., Camill, P., Veremeeva, A., and Orr, A.: Spatial heterogeneity and
 environmental predictors of permafrost region soil organic carbon stocks, *Sci. Adv.*, 7, eaaz5236,
<https://doi.org/10.1126/sciadv.aaz5236>, 2021.
- Nave, L., Johnson, K., Catharine, van I., Agarwal, D., Humphrey, M., and Beekwilder, N.: International Soil Carbon Network
 470 (ISCN) Database V3-1, International Soil Carbon Network [data set], <https://doi.org/10.17040/ISCN/1305039>, 2015.
- Onerhime, E.: Data Standards for Soil: Why aren't they taking root?, *Gates Open Res.*, 5, 74,
<https://doi.org/10.21955/gatesopenres.1116780.1>, 2021.



- Panagos, P., Van Liedekerke, M., Jones, A., and Montanarella, L.: European Soil Data Centre: Response to European policy support and public data requirements, *Land Use Policy*, 29, 329–338, <https://doi.org/10.1016/j.landusepol.2011.07.003>, 475 2012.
- Piao, S., Fang, J., Ciais, P., Peylin, P., Huang, Y., Sitch, S., and Wang, T.: The carbon balance of terrestrial ecosystems in China, *Nature*, 458, 1009–1013, <https://doi.org/10.1038/nature07944>, 2009.
- Poepplau, C., Vos, C., and Don, A.: Soil organic carbon stocks are systematically overestimated by misuse of the parameters bulk density and rock fragment content, *SOIL*, 3, 61–66, <https://doi.org/10.5194/soil-3-61-2017>, 2017.
- 480 Poggio, L., de Sousa, L. M., Batjes, N. H., Heuvelink, G. B. M., Kempen, B., Ribeiro, E., and Rossiter, D.: SoilGrids 2.0: producing soil information for the globe with quantified spatial uncertainty, *SOIL*, 7, 217–240, <https://doi.org/10.5194/soil-7-217-2021>, 2021.
- Robinson, N. J., Dahlhaus, P. G., Wong, M., MacLeod, A., Jones, D., and Nicholson, C.: Testing the public–private soil data and information sharing model for sustainable soil management outcomes, *Soil Use and Management*, 35, 94–104, 485 <https://doi.org/10.1111/sum.12472>, 2019.
- Rossiter, D. G., Liu, J., Carlisle, S., and Zhu, A.-X.: Can citizen science assist digital soil mapping?, *Geoderma*, 259–260, 71–80, <https://doi.org/10.1016/j.geoderma.2015.05.006>, 2015.
- Scharlemann, J. P., Tanner, E. V., Hiederer, R., and Kapos, V.: Global soil carbon: understanding and managing the largest terrestrial carbon pool, *Carbon Management*, 5, 81–91, <https://doi.org/10.4155/cmt.13.77>, 2014.
- 490 Shangguan, W., Dai, Y., Liu, B., Zhu, A., Duan, Q., Wu, L., Ji, D., Ye, A., Yuan, H., Zhang, Q., Chen, D., Chen, M., Chu, J., Dou, Y., Guo, J., Li, H., Li, J., Liang, L., Liang, X., Liu, H., Liu, S., Miao, C., and Zhang, Y.: A China data set of soil properties for land surface modeling, *J. Adv. Model. Earth Syst.*, 5, 212–224, <https://doi.org/10.1002/jame.20026>, 2013.
- Shangguan, W., Dai, Y., Duan, Q., Liu, B., and Yuan, H.: A global soil data set for earth system modeling, *J. Adv. Model. Earth Syst.*, 6, 249–263, <https://doi.org/10.1002/2013MS000293>, 2014.
- 495 Shi, X. Z., Yu, D. S., Warner, E. D., Pan, X. Z., Petersen, G. W., Gong, Z. G., and Weindorf, D. C.: Soil Database of 1:1,000,000 Digital Soil Survey and Reference System of the Chinese Genetic Soil Classification System, *Soil Horizons*, 45, 129, <https://doi.org/10.2136/sh2004.4.0129>, 2004.
- Soil Landscapes of Canada Working Group: Soil Landscapes of Canada version 3.2 (digital map and database at 1:1 million scale), Agriculture and Agri-Food Canada [data set], 2010.
- 500 Taylor, K. E.: Summarizing multiple aspects of model performance in a single diagram, *J. Geophys. Res.*, 106, 7183–7192, <https://doi.org/10.1029/2000JD900719>, 2001.
- Taylor, K. E.: Taylor diagram primer, 2005.



- Tian, Y., Ouyang, H., Xu, X., Song, M., and Zhou, C.: Distribution characteristics of soil organic carbon storage and density on the Qinghai-Tibet Plateau, *Acta Pedol. Sin.*, 933–942, 2008.
- 505 Tifafi, M., Guenet, B., and Hatté, C.: Large Differences in Global and Regional Total Soil Carbon Stock Estimates Based on SoilGrids, HWSD, and NCSCD: Intercomparison and Evaluation Based on Field Data From USA, England, Wales, and France: Differences in total SOC stock estimates, *Global Biogeochem Cycles*, 32, 42–56, <https://doi.org/10.1002/2017GB005678>, 2018.
- USDA-NCSS: Digital General Soil Map of U.S, U.S. Dep. of Agric. Nat. Resour. Conserv. Serv., Fort Worth, Tex. [data set],
 510 2006.
- Vitharana, U. W. A., Mishra, U., and Mapa, R. B.: National soil organic carbon estimates can improve global estimates, *Geoderma*, 337, 55–64, <https://doi.org/10.1016/j.geoderma.2018.09.005>, 2019.
- Wang, L., Zeng, H., Zhang, Y., Zhao, G., Chen, N., and Li, J.: A review of research on soil carbon storage and its influencing factors in the Tibetan Plateau, *Chin. J. Ecol.*, 38, 3506–3515, <https://doi.org/10.13292/j.1000-4890.201911.009>, 2019.
- 515 Yang, J., Li, A., Yang, Y., Li, G., and Zhang, F.: Soil organic carbon stability under natural and anthropogenic-induced perturbations, *Earth-Science Reviews*, 205, 103199, <https://doi.org/10.1016/j.earscirev.2020.103199>, 2020.
- Zhu, A., Yang, L., Fan, N., Zeng, C., and Zhang, G.: The review and outlook of digital soil mapping, *Progress in Geography*, 37, 66–78, <https://doi.org/10.18306/dlkxjz.2018.01.008>, 2018.